APPLIED AND ENVIRONMENTAL MICROBIOLOGY, Aug. 2003, p. 4413–4420 Vol. 69, No. 8
0099-2240/03/$08.00+0 DOI: 10.1128/AEM.69.8.4413–4420.2003

Multiplex Real-Time PCR for Monitoring *Heterobasidion annosum* Colonization in Norway Spruce Clones That Differ in Disease Resistance

Ari M. Hietala,* Morten Eikenes, Harald Kvaalen, Halvor Solheim, and Carl G. Fossdal

Skogforsk, 1432 Ås, Norway

Received 26 December 2002/Accepted 7 May 2003

A multiplex real-time PCR assay was developed to monitor the dynamics of the *Picea abies-Heterobasidion annosum* pathosystem. Tissue cultures and 32-year-old trees with low or high resistance to this pathogen were used as the host material. Probes and primers were based on a laccase gene for the pathogen and a polyubiquitin gene for the host. The real-time PCR procedure was compared to an ergosterol-based quantification method in a tissue culture experiment, and there was a strong correlation (product moment correlation coefficient, 0.908) between the data sets. The multiplex real-time PCR procedure had higher resolution and sensitivity during the early stages of colonization and also could be used to monitor the host. In the tissue culture experiment, host DNA was degraded more rapidly in the clone with low resistance than in the clone with high resistance. In the field experiment, the lesions elicited were not strictly proportional to the area colonized by the pathogen. Fungal colonization was more restricted and localized in the lesion in the clone with high resistance, whereas in the clone with low resistance, the fungus could be detected until the visible end of the lesion. Thus, the real-time PCR assay gives better resolution than does the traditionally used lesion length measurement when screening host clones for resistance.

Determining the colonization rate of pathogenic fungi and other microbes in host tissues is central to phytopathological studies. One way to monitor fungal hyphae within the host is by microscopic examination of host tissue stained with fungus-specific dyes (15), but this procedure is tedious and difficult to apply in a quantitative manner. Therefore, indirect methods have been developed and applied for estimation of fungal biomass in planta.

Ergosterol (6, 14)-based assays commonly have been used to determine fungal biomass within host tissues. Ergosterol is a membrane-associated sterol that occurs almost exclusively in fungi and is degraded in dying mycelium, so it correlates well with markers for metabolic activity (22). Thus, ergosterol assays are commonly used to estimate the amount of living fungal biomass (for examples, see reference 6). In all indirect methods for estimating fungal biomass, a conversion factor (i.e., the relationship between the quantity of the measured component and the total weight of the organism) must be established. The validity of the ergosterol assay for this purpose has been questioned, as the concentration of this component may vary due to nutrient availability and colony age (3). The ergosterol method also lacks specificity and is best suited for laboratory studies, where the presence of multiple fungi can be excluded and will not interfere with the results.

PCR-based techniques can be used for sensitive and specific monitoring of phytopathogenic microbes in their natural substrates. Real-time PCR is currently a promising PCR method for quantifying DNA. The measurements are performed during the exponential phase of the reaction, when PCR efficiency is not influenced by limiting reagents, small differences in reaction components, or cycling conditions. The incorporation of probes increases the specificity relative to traditional PCR and allows the monitoring of several DNA targets in the same reaction tube (multiplex real-time PCR). As a result, real-time PCR has been increasingly used for the quantification of infectious agents (for examples, see references 9, 17, 20, 25, 27, and 28).

Heterobasidion annosum is a major root rot pathogen of conifers and causes tremendous economic losses worldwide. Within the European community, the annual losses attributed to this pathogen are estimated at 800 million € (for examples, see reference 29). A breeding program focused on disease resistance would be effective in reducing future losses. During the past decades, several conifer species have been extensively screened, particularly with stem inoculations, to identify clones that differ in resistance towards *H. annosum* (5). Lesion length and fungal isolations are commonly used in the screening process, and considerable genetic variation in resistance to *H. annosum* (24) has been found. In addition to the genetic component, season and site conditions can also affect the outcome of inoculations and complicate the analysis and interpretation of data. A more accurate monitoring method would be of value when screening host material for resistance and when assessing the impact of genetic and external factors on the outcome of inoculations. To our knowledge, no accurate method has been developed for monitoring and quantifying *H. annosum* growth in planta. The objectives of this study were (i) to develop a multiplex real-time PCR assay for quantifying *H. annosum* and Norway spruce DNA, (ii) to compare the real-time PCR with an ergosterol-based assay, (iii) to monitor colonization profiles of this pathogen under laboratory and field conditions in clonal Norway spruce material with differing resistances, and (iv) to compare the resolution of a real-time PCR assay with lesion

* Corresponding author. Mailing address: Skogforsk, Høgskoleveien 12, 1432 Ås, Norway. Phone: 47 64949049. Fax: 47 64942980. E-mail: ari.hietala@skogforsk.no.

length measurements traditionally used when screening host clones for resistance. The multiplex real-time PCR assay we developed is superior in resolution to the traditional lesion length measurement.

MATERIALS AND METHODS

Norway spruce clones. The field experiment was conducted at the Hogsmark Plantation of the Norwegian Forest Research Institute, Ås, Norway. The experimental plot with spruce clones was established in a 2- by 2-m array in 1970 on a west-facing, gentle slope in a well-drained agricultural field. We used two Norway spruce clones, 409, with limited resistance to *H. annosum*, and 589, with high resistance to *H. annosum* (12).

Tissue culture experiment. For the generation of tissue culture, needles from the clones were collected in May 2000, surface sterilized in sodium hypochlorite (2% vol/vol) for 15 min, and washed in sterile deionized water. After this, the needles were plated on spruce tissue culture medium (S medium) and incubated in darkness at 24°C. After 2 to 3 weeks, a callus appeared from the basal meristem of the needles and was subcultured to fresh medium. S medium was based on inductively coupled plasma spectrophotometric analysis (19) of elements in Norway spruce seeds and gametophytes. The basal medium contained the following compounds (milligrams/liter): L-glutamine (2,000), $KH_2PO_4 \cdot 3H_2O$ (479), $MgSO_4 \cdot 7H_2O$ (468), $CaSO_4 \cdot 2H_2O$ (14), H_3PO_4 (216), $C_{12}H_{10}Mg_3O_{14} \cdot 14H_2O$ (937), $FeSO_4 \cdot 7H_2O$ (5.6), $MnSO_4 \cdot H_2O$ (70.1), H_3BO_3 (3.7), $ZnSO_4 \cdot 7H_2O$ (8.6), KI (0.25), $CoCl_2 \cdot 6H_2O$ (0.035), $Na_2MoO_4 \cdot 2H_2O$ (0.36), $NiCl_2 \cdot 6H_2O$ (0.07), and $CuSO_4 \cdot 5H_2O$ (1.1). This basal medium was supplemented with 2,4-dichlorophenoxyacetic acid (2.2 mg/liter, D-2128; Sigma, St. Louis, Mo.), 6-benzylaminopurine (1.125 mg/liter, B-9395; Sigma), *m*-inositol (1,000 mg/liter), thiamine · HCl (0.1 mg/liter), pyridoxine · HCl (0.05 mg/liter), nicotinic acid (0.05 mg/liter), glycine (0.2 mg/liter), and sucrose (10,000 mg/liter); solidified with Phytagel (3,000 mg/liter, P-8169; Sigma); and prepared as described by Kvaalen and Solheim (12).

Heterokaryotic strain 87-257/1 of *H. annosum* from the S intersterility group was used for all studies. Prior to inoculation, the fungus was cultured on S medium for 11 days in darkness at 21°C. For inoculation, host tissue pieces, 200 to 300 mg (fresh weight), were placed on the margin of actively growing fungal colonies and incubated at 21°C for 24 h. The host tissue pieces were transferred to fresh medium and placed such that the area that had been in direct contact with mycelia was facing upwards and the fungus had no immediate contact with the growing medium. Incubation was continued at 21°C for 6 days, and samples, four replicates per clone at each time, were taken at 1, 3, and 6 days after inoculation. Tissue samples were weighed and then stored at −150°C. To determine the conversion factor for the ergosterol assay and to obtain fungal DNA for real-time PCR, the pathogen was cultured on a cellophane membrane on the S medium and on malt extract agar (2% malt extract, 1.5% agar) for 11 days at 21°C.

Field experiment. Two 32-year-old ramets were employed for each clone; the four trees used were located next to each other, thus minimizing the variation in microclimatic and edaphic conditions. Prior to inoculation, the fungus was grown on malt extract agar (1% malt extract, 1.5% agar) for 7 days. Stems were inoculated 1 m above ground level by excising a plug of bark down to the sapwood surface with a 5-mm-diameter cork borer. A similarly sized plug of agar containing the actively growing fungus was inserted into the hole, and the bark plug was replaced. Three inoculations were made per ramet. After 35 days, a rectangular strip (2 by 10 cm) of bark containing phloem and cambium, with the inoculation site in the middle, was removed. Immediately after excision, the sample was frozen in liquid nitrogen and stored at −150°C. The lesion length was recorded, and the upper half of one representative lesion per ramet was sampled for DNA isolation and real-time PCR. Prior to sampling, the rhytidome and periderm were removed. The lesion was divided into sections (length, 2 mm; width, 5 mm; depth, approximately 3 mm), which were processed individually to obtain the fungal colonization profile within the lesion.

DNA isolation and quantification. Fresh tissue (tissue culture or fungal mycelia) was ground in liquid nitrogen with a mortar and a pestle. DNA was isolated from 50 mg of liquid nitrogen-ground powder by using a cetyltrimethylammonium bromide method (26). Pieces from the stem lesions, approximately 50 mg (fresh weight), were frozen in liquid nitrogen and ground twice for 2 min each time in an MM 300 mill (Retsch Gmbh, Haan, Germany); otherwise, the DNA isolation protocol was the same as for tissue culture and fungal mycelia. The DNA concentration was determined with a Dyna Quant Fluorometer 200 (Hoefer Scientific Instruments, San Fransisco, Calif.). The DNA-binding dye bisbenzimide Hoechst 33258 (Calbiochem, Darmstadt, Germany) and the reference, calf thymus DNA standard (D 0805; Sigma), were used according to the manufacturer's instructions.

Oligonucleotide primers and probes for real-time PCR. The primers and probes were designed with the Primer Express software, version 1.5a, provided with the Applied Biosystems (Foster City, Calif.) real-time quantitative PCR system. For the *H. annosum* S type, primers and probes were designed for a laccase gene (GenBank accession number HA16951). A polyubiquitin gene (GenBank accession number PAB271129) was used as the target for Norway spruce. The designed laccase forward primer, 5′-CCAGAAAGTAGACAATTA TTGGATTCG-3′, and reverse primer, 5′-GAGTTGCGGCCATTATCGA-3′, amplify the region from base 662 to base 736. The corresponding TaqMan probe, 5′-AGCGCCCAACACAGTACCCCCG-3′, lies between bases 692 and 713 in this gene. The designed polyubiquitin forward primer, 5′-TGGTCGTACTCTG GCCGATTATA-3′, and the reverse primer, 5′-ACACCTAGCGGCACACAG TTAA-3′, amplify the region from base 684 to base 780. The corresponding probe, 5′-TGCTCCGTCTCCGTGGTGGCT-3′, lies between bases 737 and 757. The laccase and polyubiquitin probes were labeled at the 5′ end with the fluorescent reporter dyes 6-carboxyfluorescein (FAM) and VIC, respectively, and both were labeled at the 3′ end with the quencher dye, 6-carboxy-tetramethylrhodamine (TAMRA). The primers and probes were ordered from ABI PRISM Primers and TaqMan Probes Synthesis Service.

PCR conditions and fluorescence detection. Each 25-μl PCR was performed in TaqMan Universal PCR master mix (P/N 4304437; Applied Biosystems). The mix is optimized for the real-time PCR assay with TaqMan probes and contains AmpliTaq Gold DNA polymerase, AmpErase UNG (uracil-*N*-glycosylase), deoxynucleoside triphosphates with dUTP, and a passive reference for normalizing the reporter fluorescence. The AmpErase UNG prevents the reamplification of any carryover PCR products containing uracil (13). Optimization of primer and probe concentrations, in order to minimize the interference from competing reactions during multiplex PCR, was performed on samples with both host and fungal material present in known concentrations at a range of dilutions. Primer concentrations of 900, 300, 150, 90, and 60 nM and probe concentrations of 500, 333, 250, and 111 nM were tested for both targets, both in single (data not shown) and in multiplex PCR. The primer concentrations selected were those that gave the lowest ΔRn (normalized reporter fluorescence) values while the cycle threshold (ΔCt; ΔCt determines the PCR cycle at which the reporter fluorescence exceeds that of the background) remained constant, i.e., 250 nM laccase probe, 90 nM concentrations of each laccase primer, 333 nM polyubiquitin probe, and 150 nM concentrations of each polyubiquitin primer. These primer-probe concentrations were tested both in single (data not shown) and in multiplex PCR.

For all PCRs, whether from standard or inoculated tissue, 25 ng of DNA in 5 μl of Tris-EDTA buffer was used as the template. The standard curve was constructed from known amounts of host and pathogen DNA. For the host, the DNA was isolated from uninoculated tissue, and for the fungus, it was obtained from malt extract agar-grown mycelium. The amounts of host and pathogen DNA used (in nanograms) were: 0 and 25, 0.9 and 24.1, 5 and 20, 12.5 and 12.5, 20 and 5, 23.75 and 1.25, 24.9 and 0.0125, 25 and 0.00125, and 25 and 0. These standard samples were included as duplicates in each PCR run.

PCR cycling parameters were 50°C for 3 min for UNG enzyme activity, 95°C for 10 min to denature the UNG enzyme and to activate the polymerase, and 40 cycles of 95°C for 15 s and 60°C for 1 min. Real-time detection of fluorescence emissions was performed with an ABI PRISM 7700 (Applied Biosystems). Data acquisition and analysis were performed with Sequence Detection System, version 1.7a, Software Package (Applied Biosystems).

Specificity of primers and probes. For testing the specificity of the primer-probe sets used, three S, F, and P type strains of *H. annosum* were grown on a cellophane membrane on malt extract agar for isolation of DNA. Strains representing *Heterobasidion araucariaceae*, *Heterobasidion insulare*, *Armillaria borealis*, *Climacocystis borealis*, *Phlebiopsis gigantea*, *Resinicium bicolor*, *Stereum sanguinolentum*, and *Trichaptum abietinum* also were included. For this testing, the same multiplex PCR conditions were applied as for infected host material.

Ergosterol. For tissue culture and mycelia, 50-mg and 5- to 10-mg aliquots of liquid nitrogen-ground powder, respectively, were used for an ergosterol assay (14). The ground tissue material was extracted twice with 500 μl of cold (4°C) absolute ethanol. The supernatants were pooled, adjusted to 1.0 ml, filtered through 0.45-μm-pore-size nitrocellulose filters (Sartorius, Paris, France), and stored at −22°C. An Agilent 1100 chromatographic system with a Merck Hitachi L4250 UV/VIS Detector operating at 280 nm was used. Separations were obtained by using a 5-μm Supelcosil LC 318 column (5 cm by 4.6 mm, inner diameter) with a 5-μm Supelcosil LC 318 guard column (2 by 4.6 cm, inner diameter) (Supelco, Bellefonte, Pa.). Elution was obtained with 100% methanol at a flow rate of 0.8 ml min^{-1}. The ergosterol peak eluted at approximately 2.5

TABLE 1. Detection of tester strains with the laccase primer-probe set[a]

Code	Species (IS group)	Host	Location	Ct value for:		Rn value for:	
				Repl. 1	Repl. 2	Repl. 1	Repl. 2
87-257/1[b]	*H. annosum* (S)	*Picea abies*	Hurum, Norway	19.9	20.6	0.80	0.72
98-1615/2	*H. annosum* (S)	*Picea abies*	Ås, Norway	20.8	21.1	0.69	0.68
73-62/18	*H. annosum* (S)	*Picea abies*	Hamar, Norway	21.1	20.7	0.66	0.65
95016	*H. annosum* (F)	*Abies alba*	Monte Amiata, Italy	20.3	20.7	0.80	0.72
95331	*H. annosum* (F)	*Picea abies*	Klein Krottenbachtal, Austria	20.0	20.1	0.69	0.68
94235	*H. annosum* (F)	*Abies alba*	Wegierska Gorka, Poland	20.6	20.4	0.65	0.69
90/171a	*H. annosum* (P)	*Pinus sylvestris*	Örvella, Notodden, Norway	28.5	28.3	0.28	0.21
60-151	*H. annosum* (P)	*Pinus elliottii*	Cordele, Ga.	29.6	30.5	0.16	0.14
60-156	*H. annosum* (P)	*Pinus pinaster*	Forte dei Marmi, Italy	30.7	30.4	0.11	0.11
96009	*H. araucariaceae*	*Araucaria cunninghamii*	Woitabe, Papua New Guinea	28.7	31.3	0.23	0.13
99045	*H. insulare*	*Keteleeria* sp.	Yunnan, Kunming, China	30.7	30.2	0.11	0.11
97-651/2	*A. borealis*	*Picea abies*	Rauma, Norway	40.0	40.0	0.00	0.00
1096/2	*C. borealis*	*Picea abies*	Ås, Norway	40.0	40.0	0.00	0.00
77-90/2	*P. gigantea*	*Picea abies*	Hurdal, Norway	40.0	40.0	0.00	0.00
83-191/1	*R. bicolour*	*Picea abies*	Follum, Norway	40.0	40.0	0.00	0.00
99-147/12	*S. sanguinolentum*	*Picea abies*	Moskog, Norway	40.0	40.0	0.00	0.00
1246/5	*T. abietinum*	*Picea abies*	Ås, Norway	40.0	40.0	0.00	0.00

[a] Template, 2.5 ng; annealing temperature, 60°C. Repl., replicate.
[b] The F type and *H. araucariaceae* and *H. insulare* strains are from the Finnish Forest Research Institute; all other strains are from Skogforsk.

min. The calibration curve was obtained by injecting ergosterol standards of known concentrations in the range of 0.1 to 40 ng μl^{-1}.

Statistical analyses. The real-time PCR, DNA yield, and ergosterol data obtained were subjected to analysis of variance by using the GLM procedure of SAS (21). In addition, product moment correlation and Spearman rank correlation between the real-time PCR, DNA yield, and ergosterol data were calculated by using the Corr procedure of SAS. Differences were considered significant at P values of <0.05.

RESULTS

Specificity of primer-probe sets. The laccase set amplified the S and F type strains with equal efficiency (Table 1), resulting in comparable ΔCt and ΔRn values. The set also recognized the P type and the two other *Heterobasidion* species, but the ΔCt values were considerably higher and the ΔRn values were correspondingly lower. When the annealing temperature was raised to 63°C, the S and F type still yielded comparable ΔCt values, but the P type and the other *Heterobasidion* species were no longer amplified. The laccase primer-probe set did not amplify host DNA or DNA from any of the other tested fungi. The polyubiquitin primer-probe set did not amplify any of the tested fungi but efficiently amplified spruce DNA.

Multiplex real-time PCR: ΔCt- and ΔΔCt-based calculation. A standard curve was constructed based on the relationship of ΔCt values and the amount of template generated from known host and pathogen DNA concentrations in multiplex PCR (Fig. 1). Host and fungal DNA were reproducibly detected over the concentration ranges used, 0.9 to 25 ng and 0.00125 to 25 ng, respectively.

We compared two protocols for predicting the amount of fungal DNA from the known samples for the standard curve. In the ΔCt-based calculation, log-transformed pathogen and host DNA concentrations were the dependent variables and the respective ΔCt values were the independent variables. To obtain the pathogen-to-total DNA ratio, the calculated amount of fungal DNA was divided by the calculated total DNA (host DNA plus fungal DNA). In the ΔΔCt-based calculation, the percentage of fungal DNA was the dependent variable and the difference between the ΔCt values of plant and fungal DNA was the independent variable. A sigmoid curve with five parameters was fitted to the data by using the Marquardt-Levenberg algorithm in the curve-fitting module of Sigma Plot, SPSS Inc. (Fig. 1C). The ΔCt method was more accurate for calculating concentrations of *H. annosum* DNA below 0.05%, whereas the ΔΔCt method was more accurate at fungal concentrations of 5 to 50% (Table 2). At the lowest calibration point (0.005% *H. annosum* DNA), the ΔΔCt method underestimated the target and predicted a negative value of −0.012, whereas ΔCt predicted a value of 0.004.

Real-time PCR, DNA yield, and ergosterol estimates in inoculated tissues. The amounts of pathogen and host DNA in the inoculated tissue samples were calculated by using the ΔCt-based calculation procedure, with equations derived from the standard curve of the same PCR run. The tissue cultures of both clones became increasingly macerated, showing a necrotic

TABLE 2. The amount of templates loaded for the standard curve in multiplex real-time PCR, the predicted values of *H. annosum* DNA using the ΔCt- and ΔΔCt-based calculation methods, and the coefficient of variation for the respective methods at the various *H. annosum* DNA percentages

Amt (ng) of host DNA loaded onto template	% *H. annosum* DNA	Amt of template estimate for calculation method based on:			
		ΔCt		ΔΔCt	
		% *H. annosum* DNA	% CV[a]	% *H. annosum* DNA	% CV
25	0.005	0.004	36	−0.012	−20
24.9	0.05	0.05	4.9	0.048	4.4
23.75	5	5.7	3.8	5.1	4.3
20	20	23	0.8	20	1.4
12.5	50	54	6.3	50	8.6
5.0	80	79	2.2	79	3.1
0.9	96.4	95	0.3	96	0.3

[a] CV, coefficient of variation.

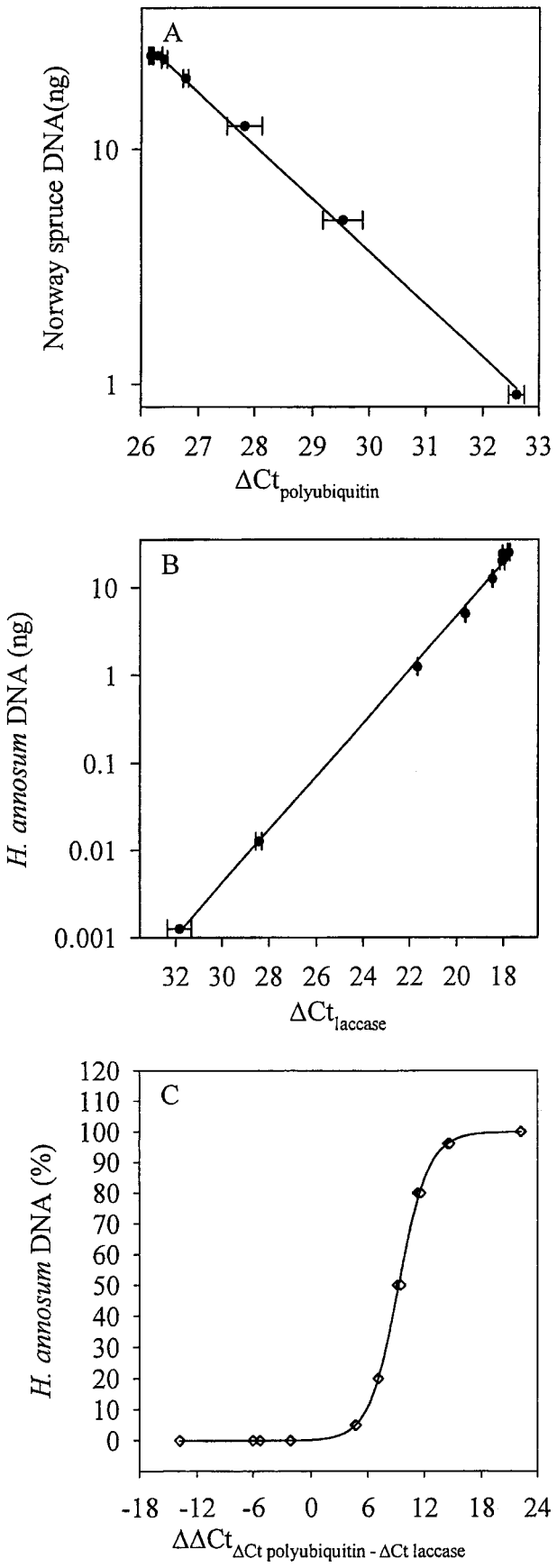

FIG. 1. Standard curves for Norway spruce and *H. annosum* DNA from multiplex real-time PCR from one PCR run. ΔCt values were plotted against log-transformed DNA amounts, and linear regression equations were calculated for the quantification of unknown samples by interpolation. (A) Standard curve for Norway spruce DNA [$\log y = (7.313 - 0.225)\, x$]. The linear regression coefficient (r^2) is 0.997. (B) Standard curve for *H. annosum* DNA [$\log y = (6.773 - 0.305)\, x$]. The linear regression coefficient (r^2) is 0.998. (C) ΔΔCt values (the laccase ΔCt value was subtracted from the polyubiquitin ΔCt value) were plotted against the percentage of *H. annosum* DNA present in the standard sample, and the sigmoid equation $y = 0.0185 + 99.9141/\{1 + \exp[-(x - 9.2321)/1.5934]\}^{1.0261}$ was calculated for the quantification of unknown samples by interpolation. The regression coefficient (r^2) is 0.999.

TABLE 3. Product moment and Spearman rank correlation coefficients between real-time PCR, ergosterol assay, and relative host DNA yield

Method	Correlation coefficient with[a]:		
	Real-time PCR	Ergosterol assay	Host DNA yield
Real-time PCR		0.908	−0.578
Ergosterol assay	0.938		−0.715
Host DNA yield	−0.648	−0.772	

[a] Values above the diagonal are product moment correlation coefficients, and values below the diagonal are Spearman rank coefficients.

appearance after day 1. On days 1 and 3 postinoculation, the amount of *H. annosum* DNA was comparable in both clones, but by day 6, clone 409 had significantly higher levels of *H. annosum* DNA ($P = 0.002$) (Fig. 2A).

Ergosterol was also measured in all tissue pieces analyzed by real-time PCR. No ergosterol was found in uninoculated control tissue. The same pattern was obtained for the ergosterol levels as with real-time PCR (Fig. 2B), with no clear differences between the clones on days 1 and 3 and significantly higher ergosterol levels for clone 409 ($P = 0.001$) on day 6. To estimate conversion factors for ergosterol, the fungal strain was grown on S and malt extract agar media and found to contain 0.42 ± 0.02 μg and 0.70 ± 0.09 μg of ergosterol per mg of fresh weight mycelium, respectively.

The total DNA yield was used to evaluate the degradation of the host DNA. The proportion of host DNA in the total DNA was estimated with the polyubiquitin primer-probe set, and this estimate was divided by the DNA yield from uninoculated control tissues to obtain the relative amount of host DNA. For day 1, the amount of host DNA yield in inoculated tissues was comparable to that in uninoculated tissues (Fig. 2C). After day 1, the amount of host DNA declined more rapidly and to a lower level in clone 409, but the differences between the two clones were not statistically significant.

The correlations between real-time PCR values and the amount of ergosterol were strong in the tissue culture experiment (Table 3). For example, no ergosterol was detected in two samples from clone 589 on the first harvesting day. These samples had the lowest real-time PCR-based fungal estimates. There was a moderate, but negative, correlation between the relative amount of host DNA, ergosterol, and real-time PCR

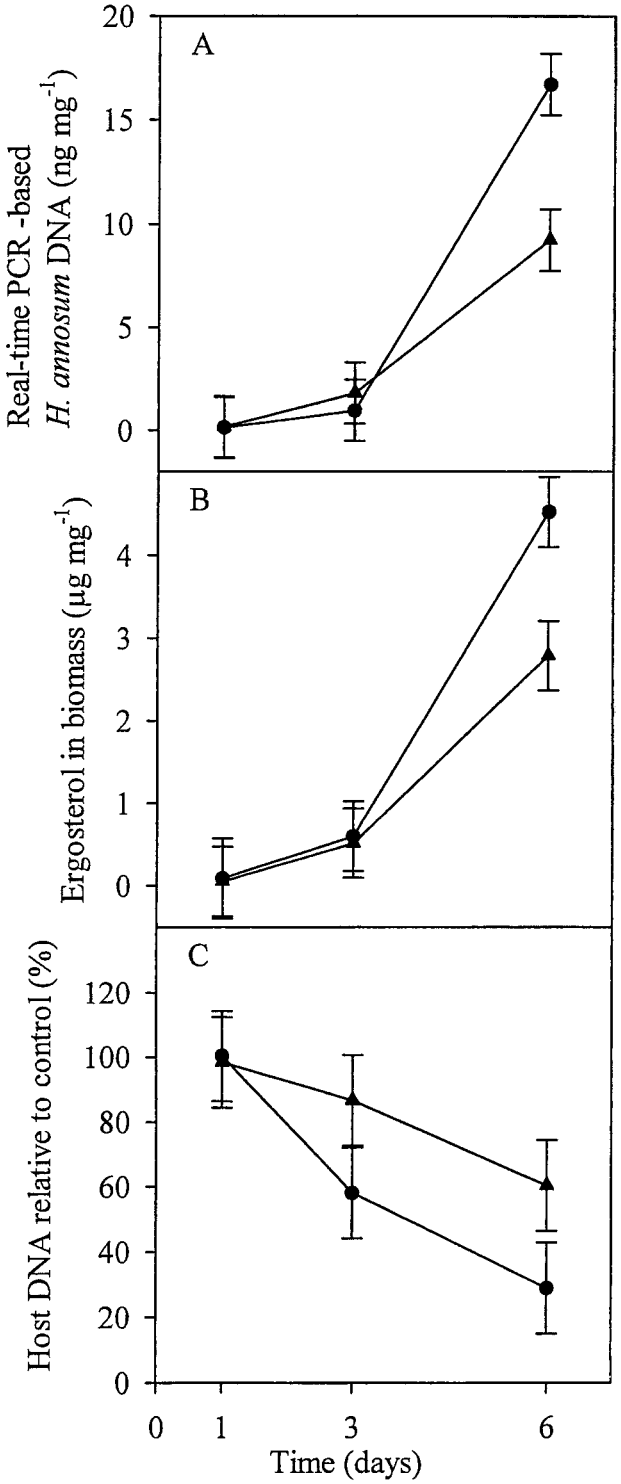

FIG. 2. The DNA and ergosterol data over the 6-day incubation period (●, clone 409; ▲, clone 589; $n = 4$ for each harvesting time/clone). (A) Amount of *H. annosum* DNA from the two clones using the ΔCt-based calculation procedure. (B) Amount of ergosterol from the two clones at different time points. (C) Relative host DNA yield (host DNA yields obtained from different time points were divided by the DNA yield obtained from uninoculated control tissues) for the two clones.

data, suggesting that host DNA degradation is associated with the degree of fungal colonization.

Colonization profiles in the lesions. Considerably larger lesions were observed in clone 409 than in clone 589 35 days after inoculation. The lesion lengths for clone 409 were 30, 15, and 26 mm (ramet 409A) and 33, 23, and 27 mm (ramet 409B). The lesion lengths for clone 589 were 8, 8, and 6 mm (ramet 589A) and 4, 5, and 6 mm (ramet 589B). The lesions in clone 589 were darker, and the interface between the lesion and (apparent) healthy tissue was sharper.

The colonization profiles of *H. annosum* differed in the two clones (Fig. 3A). In the ramets of clone 589, *H. annosum* was detected only in the 2-mm-long section next to the inoculation point, and the amount of fungus was relatively low. In the ramets of clone 409, the real-time PCR estimates indicated a gradient in the amount of fungal biomass, with the highest levels immediately adjacent to the inoculation point. In ramet 409A, fungal colonization extended to the end of the 26 mm long lesion, but in ramet 409B, fungal colonization proceeded only 10 mm from the inoculation point, even though the total lesion length was 27 mm.

The total DNA yield from DNA extractions from healthy bark of the two clones ranged between 270 and 300 ng of DNA per mg (fresh weight) of tissue (Fig. 3B). As with the real-time PCR estimates for fungal colonization, there was a gradient in total DNA yield. Even at the end of the lesions in the 409 ramets, the DNA yield was less than in the control. The total DNA yield and the amount of *H. annosum* DNA were negatively correlated ($r = -0.62$, $P = 0.0005$).

DISCUSSION

The multiplex real-time PCR assay allowed simultaneous one-tube quantification of *H. annosum* and Norway spruce DNA. With respect to the detection limit for the pathogen, the lowest point in the standard curve was 1.25 pg, but we could reproducibly detect as little as 0.5 pg of fungal DNA under comparable multiplex conditions (data not shown). The pathogen has a genome size of approximately 23 Mb (1). One nucleus of *H. annosum* thus contains approximately 0.0238 pg of DNA (1 pg of DNA = 965 Mbp) (2). The 0.5-pg detection limit equals 21 *H. annosum* nuclei. Vegetative cells of *H. annosum* are multinucleate and contain 10 to 30 nuclei (23), and the 0.5-pg limit equals 1 to 2 fungal cells. The standard curve was constructed such that at the low level of fungal DNA there was 25 ng of host DNA. A diploid nucleus of Norway spruce contains 29 pg of DNA (18). The detection limit for the *H. annosum* strain used with our multiplex conditions can be estimated as 0.5 pg of fungal DNA/25 ng of host DNA or alternatively as 1 to 2 fungal cells/860 host cells. Isozyme studies suggest the presence of multiple laccases in *H. annosum* (for examples, see reference 10). The laccase genes, however, are at present poorly characterized in this pathogen, and it is not known whether these isozymes are the products of separate laccase genes or whether they originate from differential posttranslational modifications of a single gene product. Strain-specific variation in the copy number of the target gene(s) (e.g., homokaryons versus heterokaryons) and allelic variation in the target area of the primer-probe set affect the amplification efficiency and assay sensitivity. Therefore, the calibration of the

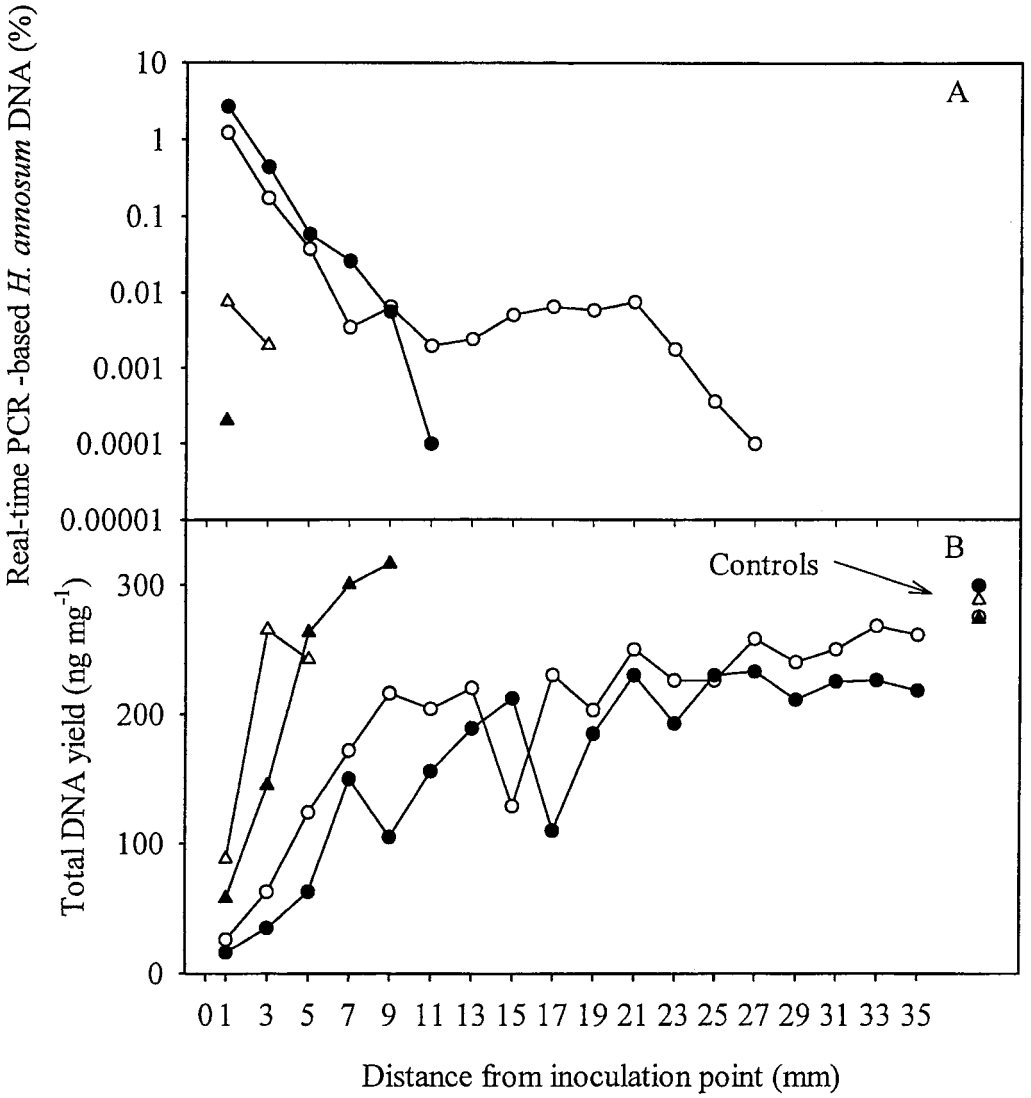

FIG. 3. DNA and real-time PCR data from the sampled lesions. The lengths of the sampled lesions for ramets 409A (○), 409B (●), 589A (△), and 589B (▲) were 26, 27, 6, and 6 mm, respectively. (A) Proportion of *H. annosum* DNA in the sampled 2-mm-long slices covering the lesions. (B) Total DNA yield from the sampled 2-mm-long slices covering the lesions.

assay (i.e., the standard curve) should be verified for each strain studied.

Both the multiplex real-time PCR and the ergosterol measurements yielded comparable data. Two tissue culture replicates of clone 589 had no detectable ergosterol on the first day after inoculation. These replicates also had the lowest, but still significant, real-time PCR estimates, indicating that the ergosterol assay is not ideal for monitoring colonization at very early stages of infection. On the other hand, the ergosterol assay is easy to perform and requires little optimization. Establishing a conversion factor to fungal biomass is problematic in both real-time PCR and ergosterol assays. As also shown here, mycelial ergosterol content varies according to cultural conditions. Real-time PCR, on the other hand, is sensitive to the number of nuclei per cell and the number of copies of the sequence per haploid genome.

Methods for quantifying a fungus under field conditions require specificity so that indigenous fungi can be excluded. The ergosterol assay we used in the laboratory experiment lacks specificity and could not be used under field conditions. With respect to the real-time PCR procedure, the host primer-probe set did not amplify any of the tested fungi. The laccase primer-probe set amplified DNA from all of the *Heterobasidion* species but from none of the common decay fungi found on Norway spruce. With respect to specificity, template purity is crucial. This matter should not be of concern in our data, as all the fungi included were processed similarly and highly diluted DNA samples were used for PCR. The ΔCt values of the *Heterobasidion* species vary considerably and in a manner consistent with ribosomal DNA-based phylogeny of the genus, in which the S and F type cannot be distinguished and the P type and the other *Heterobasidion* species are more distantly related to these two (16). Thus, the laccase primer-probe set can probably be used for accurate and reliable monitoring of natural

infection by the S or F type in areas where these two types do not coexist.

There were no clear differences in the colonization rates of the pathogen on the host clones in the tissue culture experiment within the first 3 days after inoculation, but there was considerably more host DNA degradation in clone 409 by day 3. The inoculation system allowed mycelial growth on the tissue surface that could have masked differences in the infection rates during the first 3 days. Based on the tissue culture experiment, both clones had little tolerance or resistance to *H. annosum*, even if the colonization rates at day 6 were significantly different. *H. annosum* is affected by the low levels of oxygen that characterize bark and sapwood, whereas the heartwood, the primary niche of *H. annosum*, contains the highest oxygen levels (for examples, see reference 7). Under tissue culture conditions, the partial pressure of oxygen is close to ambient (11) and thus not a limiting factor, which may have contributed to the rapid colonization by *H. annosum.*

The differential colonization profiles observed for the two clones are consistent with their ranking as resistant and susceptible clones in previous studies (4, 8, 12). In the resistant clone 589, low levels of the pathogen were observed only within the first 2 mm of tissue next to an inoculation point, whereas relatively high colonization rates were observed in clone 409. In addition, the pathogen grew from 10 to 26 mm away from the inoculation point in the 409 ramets. In clone 589, the DNA yield rose rapidly to levels comparable to those in healthy control tissue, whereas in clone 409, the DNA yield increased less rapidly and was slightly reduced relative to the control along the entire lesion. There was a negative correlation between DNA yield and real-time PCR estimates for fungal colonization, with host cell death induced by the pathogen as the most probable explanation for the low DNA yield in the lesion.

Our ultimate aim is to understand the mechanisms underlying host resistance. The colonization profiles obtained by real-time PCR can be used to assess the impact of differential expression of defense-related genes, oxygen levels, and time of season, etc., on pathogen colonization rates. Further progress also requires homogeneous host material, i.e., somatic clones, rooted cuttings, controlled crosses, or the mature clonal trees used in this study. Unfortunately mature clonal trees are rarely available for study. Tissue culture offers an alternative for resistance testing, but modification of the experimental conditions to reduce oxygen levels and limit superficial mycelial growth on the tissue surface is required to better mimic conditions prevailing within phloem and wood.

The clones we studied were chosen on the basis of previous studies regarding their resistance to *H. annosum.* The symptoms (i.e., lesion length) elicited by *H. annosum* were not fully proportional to the extent of pathogen colonization, as there were considerable differences between the lesion lengths and the extent of fungal colonization. The multiplex real-time PCR assay we developed offers an accurate tool for monitoring *H. annosum* colonization in Norway spruce. In a standard real-time PCR assay plate, up to 384 samples can be processed in a single PCR run, and the results are ready in 2 h. The sensitivity, accuracy, and high throughput nature of the real-time PCR assay will enable efficient and reliable screening of large amounts of host material.

ACKNOWLEDGMENTS

This study was financially supported by the Academy of Finland (grant to Ari Hietala) and by the Norwegian Research Council.

We thank Inger Heldal for assistance in processing the samples, Tomas Gustavsson for advice in selecting probes for real-time PCR, and Kari Korhonen for providing some of the strains.

REFERENCES

1. **Anderson, M., T. Kasuga, and K. Mitchelson.** 1993. A partial karyotype of *Heterobasidion annosum*, p. 303–313. *In* M. Johansson and J. Stenlid (ed.), Proceedings of the 8th International Conference on Root and Butt Rots. Swedish University of Agricultural Sciences, Uppsala, Sweden.
2. **Bennett, M., and J. B. Smith.** 1976. Nuclear DNA amounts in angiosperms. Philos. Trans. R. Soc. Lond. B **274:**227–274.
3. **Bermingham, S., L. Maltby, and R. C. Cooke.** 1995. A critical assessment of the validity of ergosterol as an indicator of fungal biomass. Mycol. Res. **99:**479–484.
4. **Brignolas, F., B. Lacroix, F. Lieutier, D. Sauvard, A. Drouet, A.-C. Claudot, A. Yart, A. A. Berryman, and E. Christiansen.** 1995. Induced responses in phenolic metabolism in two Norway spruce clones after wounding and inoculation with *Ophiostoma polonicum*, a bark beetle-associated fungus. Plant Physiol. **109:**821–827.
5. **Delatour, C., K. von Weissenberg, and L. Dimitri.** 1998. Host resistance, p. 143–166. *In* S. Woodward, J. Stenlid, R. Karjalainen, and A. Hüttermann (ed.), *Heterobasidion annosum*—biology, ecology, impact, and control. CAB International, Oxford, United Kingdom.
6. **Ekblad, A., H. Wallander, and T. Näsholm.** 1998. Chitin and ergosterol combined to measure total and living fungal biomass in ectomycorrhizas. New Phytol. **138:**143–149.
7. **Eklund, L.** 1990. Endogenous levels of oxygen, carbon dioxide and ethylene in stems of Norway spruce trees during one growing season. Trees **4:**150–154.
8. **Franceschi, V. R., T. Krekling, A. A. Berryman, and E. Christiansen.** 1998. Specialized phloem parenchyma cells in Norway spruce (Pinaceae) bark are an important site of defence reactions. Am. J. Bot. **85:**601–615.
9. **Frederick, R. D., C. L. Snyder, G. L. Peterson, and M. R. Bonde.** 2002. Polymerase chain reaction assays for the detection and discrimination of the soybean rust pathogens *Phakopsora pachyrhizi* and *P. meibomiae*. Phytopathology **92:**217–227.
10. **Johansson, M., M. Denekamp, and F. O. Asiegbu.** 1999. Production and isozyme pattern of extracellular laccase in the S and P intersterility groups of the root pathogen *Heterobasidion annosum*. Mycol. Res. **103:**365–371.
11. **Kvaalen, H., and S. von Arnold.** 1991. Effects of various partial pressures of oxygen and carbon-dioxide on different stages of somatic embryogenesis in *Picea abies*. Plant Cell Tissue Organ Cult. **27:**49–57.
12. **Kvaalen, H., and H. Solheim.** 2000. Coinoculation of *Ceratocystis polonica* and *Heterobasidion annosum* with callus of two Norway spruce clones with different *in vivo* susceptibility. Plant Cell Tissue Organ Cult. **60:**221–228.
13. **Longo, M. C., M. S. Berninger, and J. L. Hartley.** 1990. Use of uracil DNA glycosylase to control carry-over contamination in polymerase chain reactions. Gene **93:**125–128.
14. **Martin, F., C. Delaruelle, and J.-L. Hilbert.** 1990. An improved ergosterol assay to estimate fungal biomass in ectomycorrhizas. Mycol. Res. **94:**1059–1064.
15. **Meyberg, M.** 1988. Selective staining of fungal hyphae in parasitic and symbiotic plant-fungus associations. Histochemistry **88:**197–199.
16. **Mitchelson, K., and K. Korhonen.** 1998. Diagnosis and differentiation of intersterility groups, p. 71–92. *In* S. Woodward, J. Stenlid, R. Karjalainen, and A. Hüttermann (ed.), *Heterobasidion annosum*—biology, ecology, impact, and control. CAB International, Oxford, United Kingdom.
17. **Mumford, R. A., K. Walsh, I. Barker, and N. Boonham.** 2000. Detection of potato mop top virus and Tobacco rattle virus using a multiplex real-time fluorescent reverse-transcription polymerase chain reaction assay. Phytopathology **90:**448–453.
18. **Murray, B. G.** 1998. Nuclear DNA amounts in gymnosperms. Ann. Bot. **82:**3–15.
19. **Ogner, G., T. Wickstrøm, G. Remedios, S. Gjelsvik, G. R. Hensel, J. A. Jacobsen, M. Olsen, E. Skretting, and B. Sørlie.** 1999. The chemical analysis program of the Norwegian Forest Research Institute. Norwegian Forest Research Institute. Chemical Laboratories, Ås, Norway.
20. **Qi, M., and Y. Yang.** 2002. Quantification of *Magnaporthe grisea* during infection of rice plants using real-time polymerase chain reaction and northern blot/phospoimaging analyses. Phytopathology **92:**870–876.
21. **SAS.** 1990. SAS user's guide: statistics, vol. 1, version 6. SAS Institute, Inc., Cary, N.C.
22. **Scheu, S., and D. Parkinson.** 1994. Changes in bacterial and fungal biomass C, bacterial and fungal biovolume and ergosterol content after drying, remoistening and incubation of different layers of cool temperate forest soils. Soil Biol. Biochem. **26:**1515–1525.
23. **Stenlid, J., and A. D. M. Rayner.** 1991. Patterns of nuclear migration and heterokaryosis in pairings between sibling homokaryons of *Heterobasidion annosum*. Mycol. Res. **95:**1275–1283.

24. **Swedjemark, G., J. Stenlid, and B. Karlsson.** 1998. Genetic variation among clones of *Picea abies* in resistance to growth of *Heterobasidion annosum*. Silvae Genet. **46:**369–374.
25. **Vandermark, G. J., B. M. Barker, and M. A. Gritsenko.** 2002. Quantifying *Aphanomyces euteiches* in alfalfa with a fluorescent polymerase chain reaction. Phytopathology **92:**265–272.
26. **Walter, C., L. J. Grace, S. S. Donaldson, J. Moody, J. E. Gemmel, S. van der Maas, H. Kvaalen, and A. Lönneborg.** 1999. A highly efficient biolistic transformation protocol for *Picea abies* (L.) Karst. embryogenic tissue and regeneration of transgenic plants. Can. J. For. Res. **29:**1539–1546.
27. **Weller, S. A., J. G. Elphinstone, N. C. Smith, N. Boonham, and D. E. Stead.** 2000. Detection of *Ralstonia solanacearum* strains with a quantitative multiplex, real-time, fluorogenic PCR (TaqMan) assay. Appl. Environ. Microbiol. **66:**2853–2858.
28. **Winton, L. M., J. K. Stone, L. S. Watrud, and E. M. Hansen.** 2002. Simultaneous one-tube quantification of host and pathogen DNA with real-time polymerase chain reaction. Phytopathology **92:**112–116.
29. **Woodward, S., J. Stenlid, R. Karjalainen, and A. Hüttermann. (ed.).** 1998. *Heterobasidion annosum*—biology, ecology, impact, and control. CAB International, Oxford, United Kingdom.